

Using ^{19}F NMR to Investigate Cationic Carbon Dot Association with Per- and Polyfluoroalkyl Substances (PFAS)

Riley E. Lewis, Cheng-Hsin Huang, Jason C. White, and Christy L. Haynes*

Cite This: *ACS Nanosci. Au* 2023, 3, 408–417

Read Online

ACCESS |



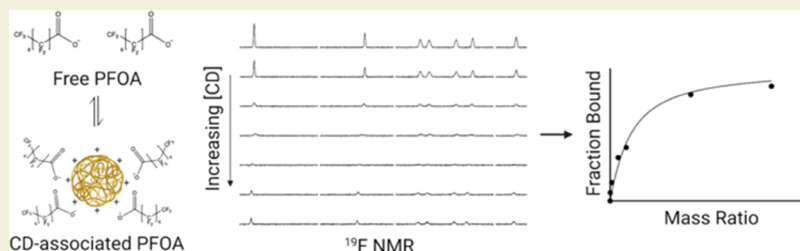
Metrics & More



Article Recommendations



Supporting Information



ABSTRACT: There is much concern about per- and polyfluoroalkyl substances (PFAS) based on their environmental persistence and toxicity, resulting in an urgent need for remediation technologies. This study focused on determining if nanoscale polymeric carbon dots are a viable sorbent material for PFAS and developing fluorine nuclear magnetic resonance spectroscopy (^{19}F NMR) methods to probe interactions between carbon dots and PFAS at the molecular scale. Positively charged carbon dots (PEI-CDs) were synthesized using branched polyethyleneimine to target anionic PFAS by promoting electrostatic interactions. PEI-CDs were exposed to perfluorooctanoic acid (PFOA) to assess their potential as a PFAS sorbent material. After exposure to PFOA, the average size of the PEI-CDs increased (1.6 ± 0.5 to 7.8 ± 1.8 nm) and the surface charge decreased ($+38.6 \pm 1.1$ to $+26.4 \pm 0.8$ mV), both of which are consistent with contaminant sorption. ^{19}F NMR methods were developed to gain further insight into PEI-CD affinity toward PFAS without any complex sample preparation. Changes in PFOA peak intensity and chemical shift were monitored at various PEI-CD concentrations to establish binding curves and determine the chemical exchange regime. ^{19}F NMR spectral analysis indicates slow-intermediate chemical exchange between PFOA and CDs, demonstrating a high-affinity interaction. The α -fluorine had the greatest change in chemical shift and highest affinity, suggesting electrostatic interactions are the dominant sorption mechanism. PEI-CDs demonstrated affinity for a wide range of analytes when exposed to a mixture of 24-PFAS, with a slight preference toward perfluoroalkyl sulfonates. Overall, this study shows that PEI-CDs are an effective PFAS sorbent material and establishes ^{19}F NMR as a suitable method to screen for novel sorbent materials and elucidate interaction mechanisms.

KEYWORDS: PFAS, carbon dots, ^{19}F NMR, sample preparation, sorption, affinity

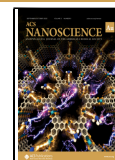
INTRODUCTION

Effective remediation strategies for per- and polyfluoroalkyl substances (PFAS) are necessary due to their environmental persistence and numerous negative health implications.^{1–3} The typical structure of PFAS includes a fluorinated carbon chain and polar head group, which renders these molecules very stable and amphiphilic, posing numerous challenges for remediating PFAS-contaminated environmental matrices.^{2,4,5} Adsorption technologies have emerged as one promising method for removing PFAS.^{6–8} Activated carbon is one of the most widely used sorptive materials; however, while proven effective for long-chain PFAS species, it is typically less effective for shorter-chain PFAS species and can be compromised by natural organic matter and inorganic ions.^{8,9} Investigations into the mechanisms driving PFAS sorption indicate materials with the potential for both electrostatic and hydrophobic interactions show the most promise for effectively removing a wide range of PFAS species.^{7,9,10} As a result,

developing cost-effective sorbent materials with affinity for a wide range of PFAS is critical to establish effective remediation techniques.

Carbon dots (CDs) are a broad class of nanomaterials with great potential as a PFAS sorbent based on their use of inexpensive precursors, tunable surface chemistry, and facile synthesis.^{11,12} Within the category of CDs, there are graphene quantum dots, carbon quantum dots, and amorphous/polymeric carbon dots; amorphous/polymeric CDs have the advantages that they are frequently synthesized at low temperatures and can be synthesized from a range of polymer

Received: May 26, 2023
Revised: August 4, 2023
Accepted: August 4, 2023
Published: August 25, 2023



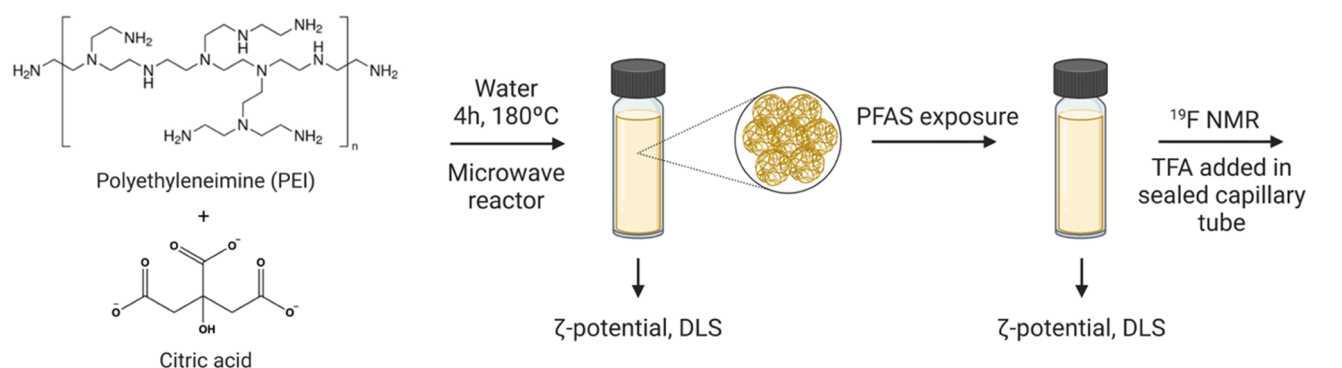


Figure 1. Schematic of PEI-CD synthesis and PFAS exposure experiments.

and small-molecule precursors.¹³ Synthesis from a range of precursors facilitates a wide array of applications taking advantage of chemical affinity for various compounds,^{13,14} which can be readily extended to PFAS. The precursors used in CD synthesis can be carefully chosen to incorporate hydrophobic pockets and functional groups that promote electrostatic interactions. As noted, there is an urgent need to design materials that effectively sorb PFAS in a cost-efficient manner and allow investigations into the interactions that drive PFAS sorption. The range of CD synthetic precursors and potential for functionalization provide an excellent platform to further understand PFAS sorption while developing cost-effective remediation materials.¹⁵ To the best of our knowledge, the only instance of applying CDs to PFAS remediation systems is through incorporation into a hydrogel for perfluorooctane sulfonate (PFOS) adsorption.¹⁶ The CD hydrogels showed a much higher uptake capacity for PFOS than any other carbonaceous sorbent materials, highlighting the promise for CD-based PFAS remediation.

Assessing the effectiveness of PFAS sorbent materials is typically done using LC-MS methods and requires separation of the sorbent material from excess PFAS in solution.¹⁷ This is frequently done through centrifugation and analyzing remaining free PFAS in the supernatant. However, CDs do not readily centrifuge out of solution. Other sample cleanup methods like C₁₈ and SPE sorbents are not effective for recovering all PFAS and introduce potential points for systematic biases from sample preparation.¹⁸ Fluorine nuclear magnetic resonance spectroscopy (¹⁹F NMR) is an attractive alternative to assess CD uptake of PFAS that is nondisruptive and requires no centrifugation, chemical treatment, or other complex sample preparation steps.¹⁹ In this case, NMR analysis is possible because the carbon dot suspensions maintain colloidal stability even at high concentrations.²⁰

Fluorine NMR peak intensity and chemical shifts are very sensitive to changes in the molecular environment surrounding the fluorine atoms.²¹ As a result, chemical shift perturbations and changes in peak intensity are frequently used to identify ligand–protein binding events and quantify interactions.^{22–25} Titration experiments can reveal additional information about the system such as the chemical exchange regime, which describes the rate a nucleus goes between two or more molecular environments, such as from free to bound, and provides insight into affinity. Many ¹⁹F NMR-based experiments focus on traditional biological systems; however, recent applications have expanded to include PFAS analysis by elucidating analyte binding orientations,^{26–28} assessing degradation,^{29,30} and quantification of total PFAS in environmental

samples.^{18,31} To the best of our knowledge ¹⁹F NMR has not been used to quantify PFAS affinity for sorbent materials before this work. We can further expand ¹⁹F NMR methods to a PFAS-nanoparticle system and quantify CD affinity toward PFAS, determine chemical exchange regimes, and elucidate potential binding mechanisms that inform future sorbent design.

The goals of this study were to (1) determine if CDs are an effective PFAS sorbent material and (2) develop a method to probe interactions between CDs and PFAS. To do this, CDs were designed and synthesized to target anionic PFAS. This was achieved using polyethyleneimine (PEI), a positively charged amine-rich polymer precursor, to promote electrostatic interactions and incorporate hydrophobic pockets into the CDs.³² Allowing for both electrostatic and hydrophobic interactions increases the potential for association with a wide range of PFAS and helps maintain affinity even in more complex matrices. CD size and surface charge following exposure to PFOA, an anionic PFAS with environmental relevance, were tracked to provide insight into any associations occurring between CDs and PFOA. Changes in ¹⁹F NMR PFOA peak intensity and chemical shifts during a CD titration were monitored to establish a dissociation constant (*K_D*), determine the chemical exchange regime, and elucidate potential binding mechanisms. Following the successful association between PEI-CDs and PFOA, we expanded to a 24-PFAS mixture to investigate CD performance in a more complex PFAS matrix. In total, we show CDs have great promise as a PFAS sorbent material and that ¹⁹F NMR provides an ideal background-free method to investigate PFAS sorption with no significant sample preparation.

RESULTS AND DISCUSSION

Synthesis and Characterization of PEI Carbon Dots (PEI-CDs)

Polyethyleneimine-based carbon dots (PEI-CDs) were synthesized through a hydrothermal reaction of branched polyethyleneimine (PEI) and citric acid in a microwave reactor (Figure 1). Citric acid was used as a cross-linking agent, where the carboxyl and hydroxyl groups undergo condensation reactions with the PEI amine groups. The resulting product from a standard synthesis was a translucent yellow suspension that could be lyophilized to produce ~500 mg of CD product. Dynamic light scattering (DLS) indicates that PEI-CDs have an effective hydrodynamic diameter of 1.6 ± 0.5 nm based on the number average (see Supporting Information S1 for additional size characterization data). In addition, zeta-potential

measurements show a positive charge ($+38.6 \pm 1.1$ mV), which is most likely a result of using PEI, an amine-rich precursor. Fluorescence measurements indicate the excitation/emission maxima at 350 nm/445 nm. These excitation/emission wavelengths align with other PEI-based CDs,³³ and the fluorescent nature indicates these are amorphous/polymeric carbon dots.¹³

PEI-CD Exposure to PFAS

Initial experiments were conducted to assess any changes to the size, charge, and fluorescence properties of the PEI-CDs upon exposure to 5 mg/L perfluorooctanoic acid (PFOA). PFOA was chosen as the target PFAS for initial experiments based on its environmental relevance.³⁴ After exposure to PFOA for 72 h, PEI-CDs significantly increased in effective hydrodynamic diameter from 1.6 ± 0.5 to 7.8 ± 1.8 nm (Table 1). This increase is most likely a result of PFOA sorption to

Table 1. Values for Hydrodynamic Diameter and ζ -Potential of PEI-CDs with and without PFOA

	PEI-CDs	PEI-CDs with PFOA	P-value
hydrodynamic diameter (nm)	1.6 ± 0.5	7.8 ± 1.8	<0.005
ζ -potential (mV)	$+38.6 \pm 1.1$	$+26.4 \pm 0.8$	<0.0001

PEI-CDs, resulting in a larger effective size; this change in effective size could be either an actual increase in size or an increase in mass that is reported as a change in size. The ζ -potential of the PFOA-exposed PEI-CDs significantly decreased from $+38.6 \pm 1.1$ to $+26.4 \pm 0.8$ mV, further indicating sorption as the negatively charged PFOA molecule will mask and balance some of the PEI-CD positive charge, resulting in a lower ζ -potential. Both the increase in effective size and decrease in ζ -potential of PEI-CDs in the presence of PFOA are consistent with significant analyte sorption. The fluorescence properties of the PEI-CDs did not change in a significant way following exposure to a range of PFOA concentrations. There are some slight variations in intensities

between samples but no explicit shifts in emission maxima (Figure 2). As a result, PEI-CDs are not able to act as a fluorescence sensor for PFOA, but PEI-CDs could be fluorescently tracked within biological systems even after sorption.

Understanding PFOA Sorption to PEI-CDs

To further understand the interactions occurring between PFOA and PEI-CDs, ¹⁹F NMR spectroscopy was employed to confirm sorption, assess affinity, and elucidate additional binding information. We monitored changes in chemical shift and peak intensity of PFOA across various PEI-CD concentrations and time points. If PFOA becomes associated with the PEI-CDs, there will be various changes to chemical shift and peak intensity because of the changing molecular environment of the fluorine in the PFOA. In this case, increasing amounts of PEI-CDs induced changes to the PFOA ¹⁹F NMR spectrum, further confirming sorption (Figure 3). Initially, PFOA peaks decrease in intensity until the PEI-CD concentration reaches 0.1 g/L, at which point, the PFOA peaks become very broad and low in intensity. Resonance broadening can be a result of slow and intermediate chemical exchange as PFOA is interchanging between free and CD-associated states, and is typically characteristic of higher-affinity interactions.³⁵ When PFOA becomes associated with the CDs, the CDs experience a shorter T_2 , which results in signal broadening. Additionally, the nonuniform structure of CDs provides numerous different environments for association, potentially resulting in slightly different chemical shifts and broadened peaks as multiple PFOA molecules associate with varied sites on the CDs.³⁶ As PEI-CD concentration increases beyond 0.1 g/L, new and shifted PFOA peaks appear; these new PFOA peaks continue to increase in intensity as PEI-CD concentration increases. The appearance of new PFOA peaks is consistent with a slow-intermediate chemical exchange regime, where peaks initially broaden but become sharp again in a concentration-dependent manner as the ratio of CD-associated PFOA increases.³⁵

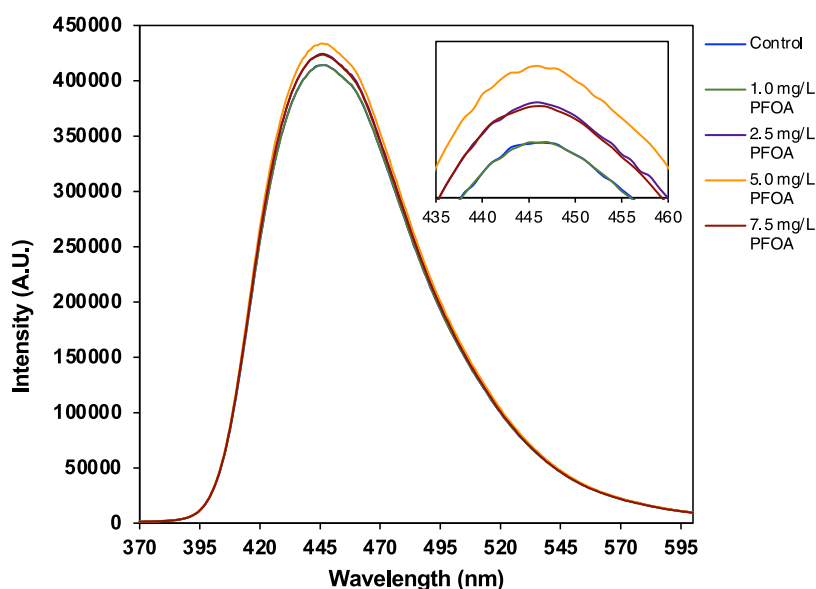


Figure 2. Fluorescence spectra ($\lambda_{\text{ex}} = 350$ nm) of PEI-CDs with varying concentrations of PFOA. The inset shows minimal differences in emission maxima or intensity.

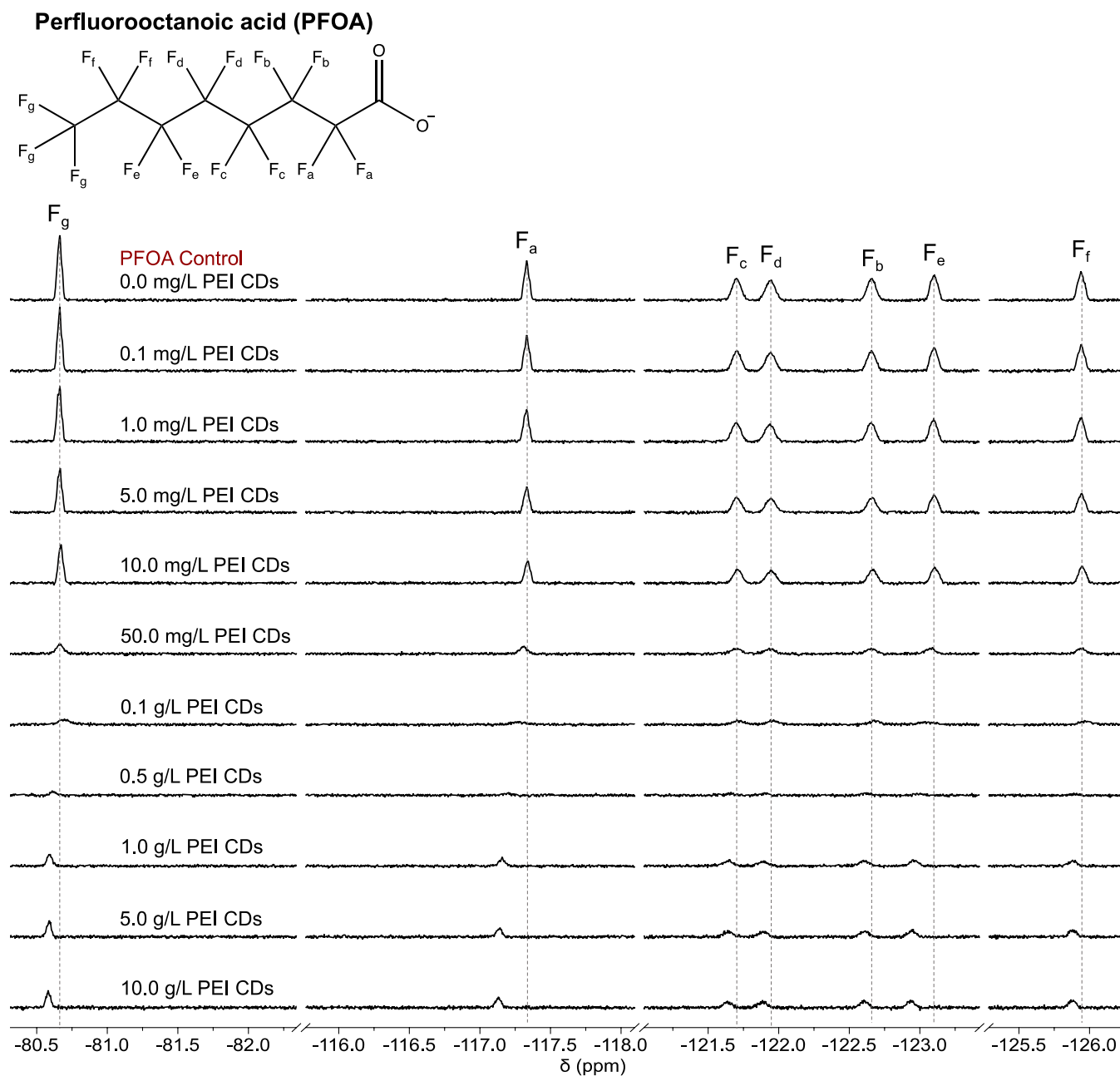


Figure 3. ¹⁹F NMR spectra of 5 mg/L PFOA with increasing concentrations of PEI-CDs after 72 h of mixing. Dashed lines are included to show changes in the chemical shift from the PFOA control, and each peak is labeled to correspond with the fluorine atoms labeled on the PFOA structure.

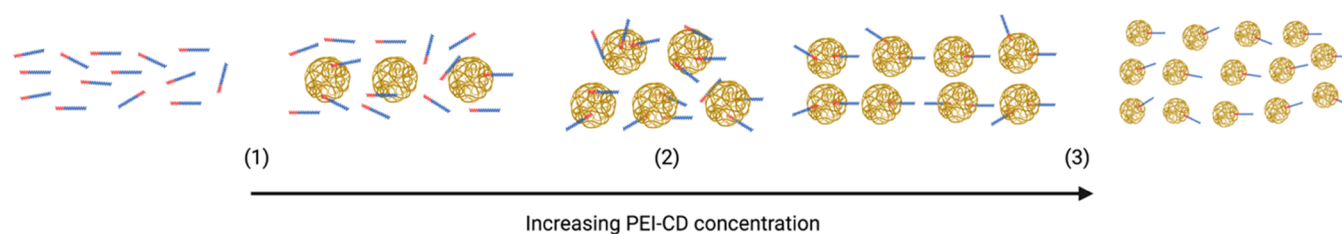


Figure 4. Visual representation of how the PFOA solution is changing with increasing PEI-CD concentration based on the changes to NMR spectra. Blue and red rods represent PFOA, and yellow circles represent PEI-CDs.

As the concentration of PEI-CDs increases, we simultaneously observe peak broadening, decreases in peak height, and changes to chemical shifts (Figure 3). This is not

surprising due to the large size and nonuniform structure of CDs, resulting in shorter T_2 values for PFOA, and numerous sorption sites with multiple mechanisms of interaction and

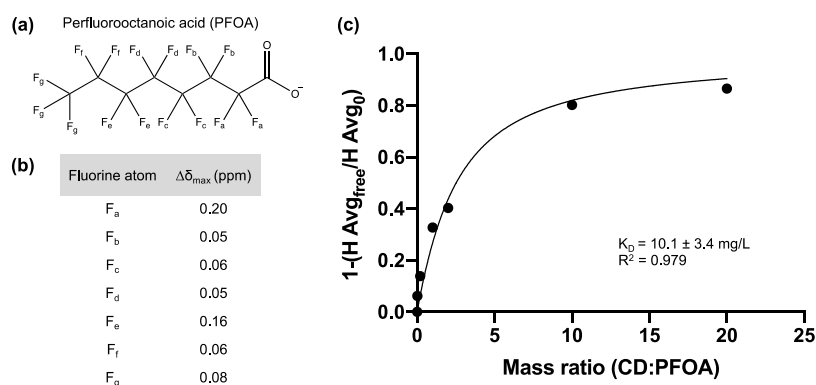


Figure 5. (a) Labeled perfluorooctanoic acid (PFOA) molecule, indicating the fluorine atoms responsible for NMR features in Figure 3. (b) Table showing the maximum change in chemical shift for each PFOA peak across the range of PEI-CD concentrations used in Figure 3. (c) Binding curve generated from the average height of all peaks in the first seven spectra of Figure 3.

Table 2. Comparison between the Percent Removal of PFOA by Other Sorbent Materials and the Estimated Percent Removal by PEI-CDs Based on the Estimated K_D Value under Varying Conditions

material	material conc.	PFOA conc.	% removal	estimated PEI-CD % removal	reference
DEXSORB	1 $\mu\text{g/L}$	10 mg/L	~10%	~50%	6
DEXSORB+	1 $\mu\text{g/L}$	10 mg/L	>99%		
Amine-CDP	1 $\mu\text{g/L}$	10 mg/L	>99%		
AE Resin	1 $\mu\text{g/L}$	10 mg/L	~50%		
PEI-f-CMC	100 $\mu\text{g/L}$	50 mg/L	~65%	~83%	32
Fe ₃ O ₄ nanoparticles on GAC	100 mg/L	500 mg/L	~60–80%	~98%	38
granular activated carbon (GAC)	100 mg/L	500 mg/L	55–60%		
powdered activated carbon (PAC)	20 mg/L	1 g/L	~51%	>99%	39
GAC	5 mg/L	10 g/L	96%	>99%	40
PAC	5 mg/L	10 g/L	>99%		
PEI-CDs	5 mg/L	100 mg/L	90%		this work

different affinities. Additionally, there are multiple environments for PFOA to exist within and in association with the PEI-CDs, resulting in a range of chemical shifts and potentially broadened peaks.

Based on the changes to the NMR spectra throughout the range of PEI-CD concentrations, we hypothesize the following pattern of sorption (Figure 4): Initially (1), there are many free PFOA molecules, and a decrease in peak height occurs as PFOA becomes associated with PEI-CDs; then at some point (2), all PFOA is associated with PEI-CDs, with many PFOA molecules on each CD, leading to shortened T_2 times, potentially many different microenvironments, and thus very broad and nearly undetectable PFOA peaks; and finally (3), as PEI-CD concentration increases further, there are less PFOA molecules per PEI-CD, and the PFOA is likely associating with sites that have higher affinity and more similar environments. At this point, new NMR features appear corresponding to the higher-affinity environments and continue to grow with additional PEI-CDs. Additional T_2 relaxation filter experiments would enhance our understanding of the interactions between PFOA and CDs and provide complementary information to this hypothesis; however, these experiments were not pursued in this report.

Further interrogation of the NMR spectra in Figure 3 reveals that the α -fluorine, which resides closest to the carboxylate group on PFOA, appears at -117.33 ppm with no PEI-CDs present, compared to -117.13 ppm with the highest PEI-CD concentration used. Changes in chemical shift are present across all fluorine atoms; however, the α -fluorine experiences the greatest change (Figure 5b). This suggests that the

chemical environment surrounding the α -fluorine changes the most, aligning with the idea that electrostatic interactions are a dominant sorption mechanism.

Determining K_D Values

The disappearance and reappearance of PFOA peaks at new chemical shifts as PEI-CD concentration increases reveal critical information about free and bound PFOA.^{22,35} However, the absence of any titration points where peaks from both bound and free PFOA are simultaneously well resolved indicates slow-intermediate exchange kinetics. It is possible that this is also a result of severe peak broadening brought about by numerous nonspecific binding sites on PEI-CDs for PFOA and the many potential microenvironments PFOA could exist within. Unfortunately, there are no straightforward methods to model materials with multiple different binding sites,^{24,37} which can be assumed to be true for PEI-CDs. Thus, to quantify binding and affinity, methods commonly used for assessing ligand–protein interactions have been adapted, assuming a slow exchange regime.²²

The K_D values were extracted from binding curves using changes to PFOA peak integration or peak height and the mass ratios of PEI-CDs:PFOA. The first seven spectra from the top of Figure 3 were used to build a binding curve, as the resonances in that CD concentration range (0–0.1 g/L) correspond to free PFOA. Binding curves were assembled for each fluorine group on PFOA to elucidate potential differences in affinity across the PFOA molecule and provide insight into binding orientations. Additionally, the average peak height at each concentration point was used to assign a general K_D value

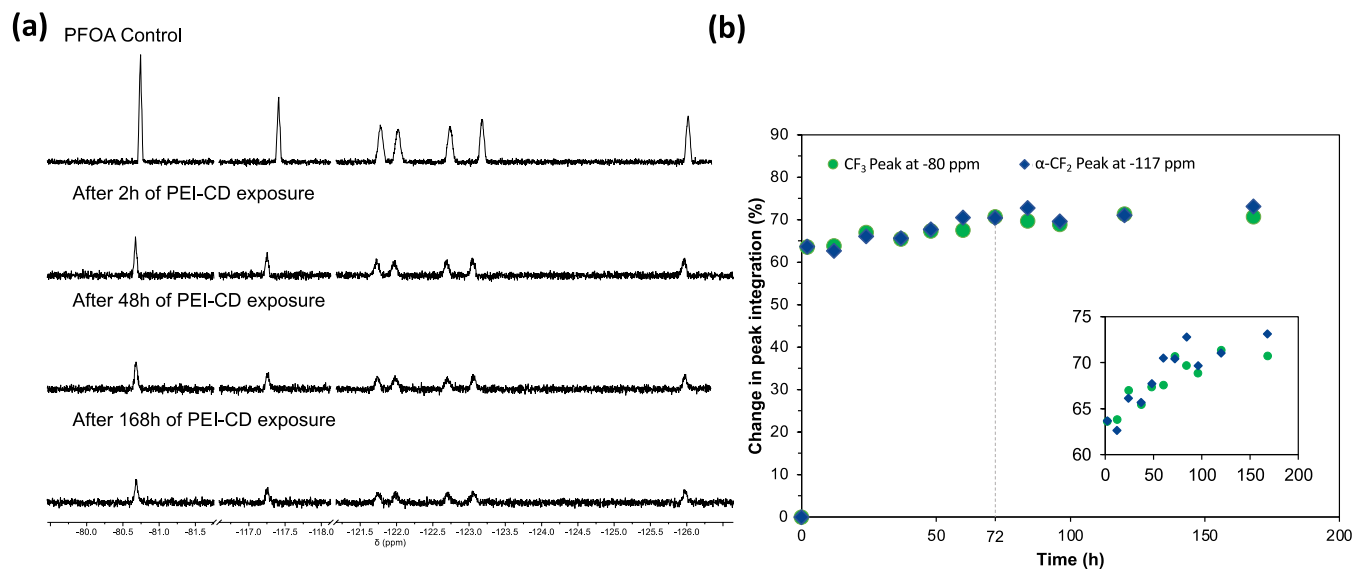


Figure 6. (a) Selected ^{19}F NMR spectra of PFOA at different time points after exposure to 100 mg/L PEI-CDs and (b) the corresponding change in peak integration at all time points compared to that without PEI-CDs for the CF_3 peak at -80.7 ppm and α -fluorine at -117.4 ppm. The inset shows a magnified version of the 2–68 h time points. The 72 h time point is noted with a vertical dashed line as that is when all other ^{19}F NMR and characterization were conducted.

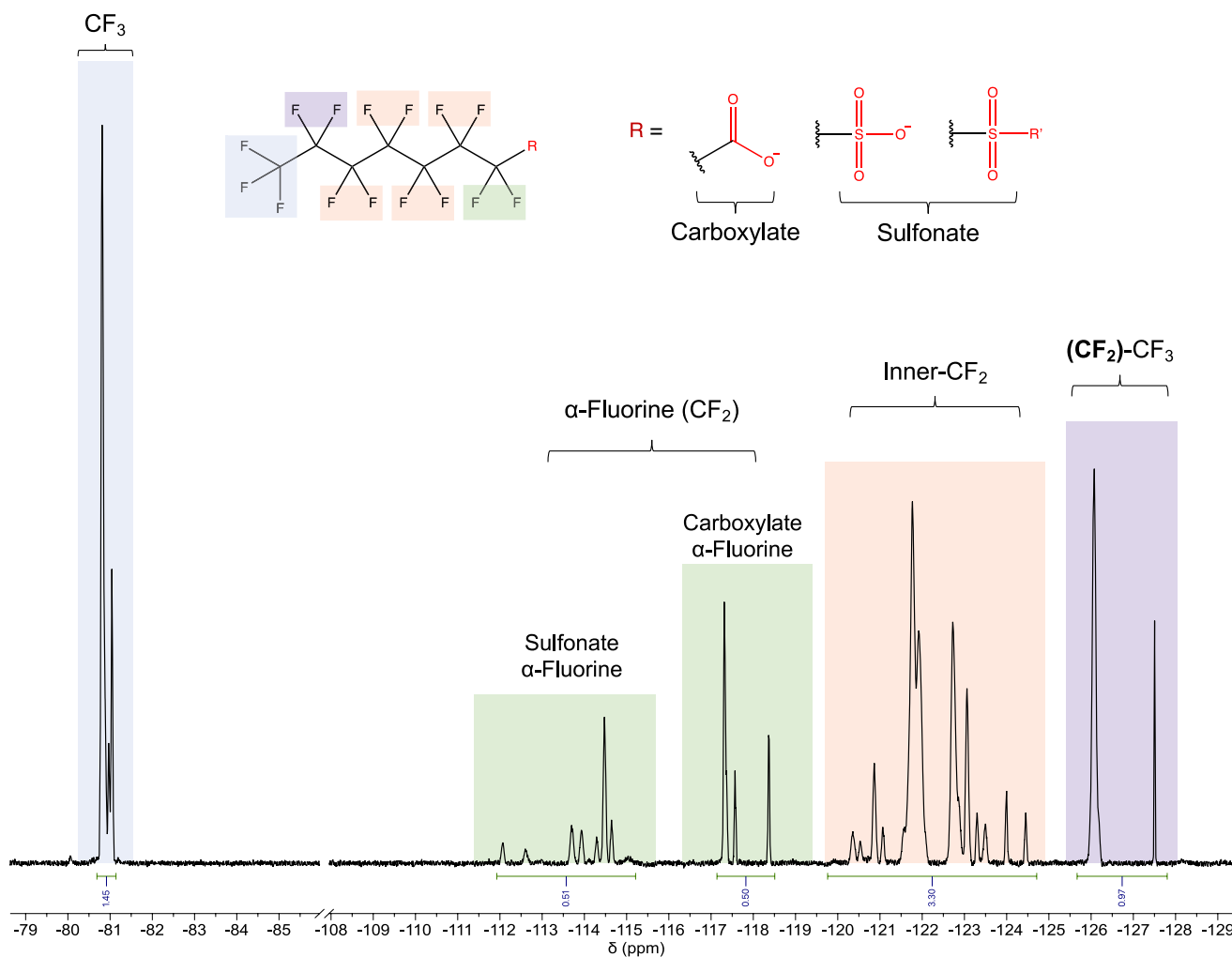


Figure 7. General peak assignments for 24-PFAS mixture.

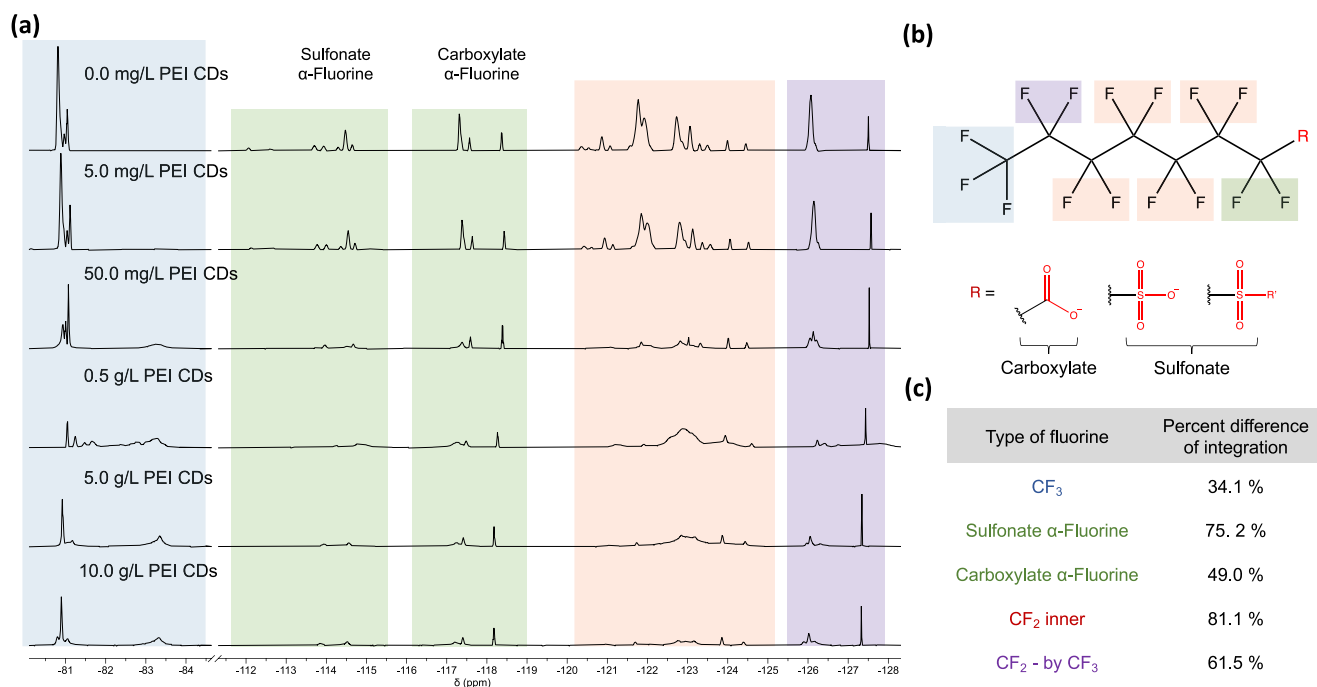


Figure 8. (a) ^{19}F NMR spectra of a 24-PFAS mixture with each component at 5 mg/L and increasing amounts of PEI-CDs. (b) General structure corresponding to the different regions identified in Figure 7. (c) Percent difference in integration between the mixture control and incubation with 10 g/L PEI-CDs for the spectral regions and structural elements highlighted.

for PFOA (Figure 5c). The bound fraction (f_b) was estimated using peak intensity (peak integration or height) during the beginning titration points where free PFOA is disappearing (0.0–100 mg/L PEI-CD) using:

$$f_b = 1 - \frac{I_{\text{free}}}{I_0}$$

where I_{free} is the PFOA peak intensity at each titration point and I_0 is the PFOA peak intensity in the absence of PEI-CDs. The overall K_D value for PEI-CDs associating with PFOA is 10.1 ± 3.4 mg/L using average peak height (Figure 5c). Comparing calculated K_D values for each fluorine group (see Supporting Information Section S3) reveals that the α -fluorine has the lowest K_D value, or highest affinity, when using either peak integration or peak height, 8.3 ± 3.7 and 12.8 ± 5.4 mg/L, respectively. The α -fluorine showing the highest affinity corresponds with it also having the greatest change in chemical shift (Figure 5b), further suggesting electrostatic interactions as the primary mechanism of sorption.

To understand how PEI-CDs compare to other sorbent materials, we can use the overall K_D value of 10.1 ± 3.4 mg/L to estimate the percent removal of PFOA under various conditions and compare that performance to previously studied materials (Table 2). PEI-CDs show a competitive predicted percent removal of PFOA in comparison to other materials and perform much better than many well-established sorbent materials, such as granular and powdered activated carbons.^{38–40} Additionally, a higher percent removal is predicted for the PEI-CDs in comparison to PEI-functionalized cellulose microcrystals at 100 $\mu\text{g/L}$ PFOA, which could be attributed to the higher surface area-to-volume ratio associated with nanoscale materials.³² Based on the K_D value of 10.1 mg/L, a system contaminated with 1 $\mu\text{g/L}$ of PFOA would need ~ 134 mg/L of PEI-CDs to remove PFOA to levels below the

USA EPA advisory concentration of 70 ng/L or ~ 2.5 g/L of PEI-CDs to remove PFOA to below the newly proposed EPA maximum contaminant level of 4.0 ng/L. Assuming the current advisory concentration of 70 ng/L, it would cost $\sim \$0.37$ /gallon to remediate water contaminated with 1 $\mu\text{g/L}$ PFOA using PEI-CDs (additional details on assumptions described in S4).

Time-Based ^{19}F NMR Experiments

To understand the timescale of PEI-CD sorption of PFOA, we examined spectral changes to PFOA features over the course of 1 week at a single concentration of PEI-CDs and PFOA and compared them to the spectral features from the pure PFOA spectrum (Figure 6). By the end of the first 2 h of 1D NMR acquisition, there was a 63% reduction in signal intensity for both the $-\text{CF}_3$ group and α -fluorine resonances in comparison to pure PFOA (Figure 6b). After 1 week, the signal reduction increased to 73 and 70% for the $-\text{CF}_3$ group and α -fluorine resonances, respectively. Based on the changes in signal intensity, most sorption occurs within the first 2 h of exposure, with some additional sorption over the following 70 h, and no significant additional sorption for the remainder of the week. Importantly, there are no obvious signs of desorption over the course of the 1-week time frame. The temporal limitations with ^{19}F NMR make it difficult to look at shorter timescales with the parameters used, and there is most likely significant information about the timescale of sorption that is unobservable in these experiments. Overall, this confirms that the 72 h time point used for kinetic studies and additional characterization is appropriate.

Exposure to 24-PFAS Mixture

To further explore PEI-CDs as a potential sorbent material, ^{19}F NMR experiments were conducted using a 24-PFAS mixture. The PFAS mixture includes those in US EPA Method 8327,

which is relevant to surface water, groundwater, and wastewater matrices. The ^{19}F NMR spectrum of the mixture was partially assigned based on previous ^{19}F NMR studies (Figure 7).³¹ Regions corresponding to five different groups were identified: the CF_3 groups, carboxylate α -fluorines, sulfonate α -fluorines, the inner CF_2 , and CF_2 next to the CF_3 . The ratios of integration values for the various regions correlated well to predicted ratios.

The PFAS mixture was exposed to increasing PEI-CD concentrations, and spectral changes were monitored (Figure 8a). Each PFAS in the mixture was set to the same concentration used in PFOA experiments, leading to 24 times the total PFAS amount. The lowest concentration of PEI-CDs used (5 mg/L) induced a slight decrease in peak intensities. At concentrations ≥ 50 mg/L PEI-CDs, the mixture spectra showed very apparent decreases in peak intensity, chemical shift changes, and peak broadening, indicating widespread sorption of PFAS. However, the peaks at -118.4 and -127.4 ppm did not undergo any intensity or chemical shift changes throughout the titration. A comparison between the ^{19}F NMR spectrum of neat perfluorobutanoic acid (PFBA) and the 24-PFAS mixture suggests these two peaks correspond to PFBA, the shortest-chain PFAS in the mixture (SI Section S5).

To further illuminate differences in association among the components of the PFAS mixture, the percent difference of integration between the PFAS mixture control and the highest PEI-CD concentration (10.0 g/L) was calculated for the various fluorine groups (Figure 8c). The CF_3 group had the lowest percent difference, aligning with the hypothesis that the most likely mechanism of interaction is through electrostatics (far from the CF_3), leading to less changes in the CF_3 group environment and thus less changes in intensity. Additionally, it is possible that the new broad peak at -83.3 ppm contributes significantly to CF_3 integration for the 10.0 g/L PEI-CD spectrum, leading to a lower percent difference. The sulfonate and carboxylate α -fluorine groups had 75.2 and 49.0% difference, respectively, suggesting that PEI-CD sorption was greater for perfluoroalkyl sulfonates in comparison to perfluoroalkyl carboxylates. This observation is consistent with previous studies⁷ that show the high-affinity sulfonates have for various sorbent materials. The inner CF_2 chain has the highest percent difference in integration with 81.1%; it is possible that PEI-CDs have greater affinity for longer-chain molecules, leading to a greater difference in mid-PFOA integration. An affinity for longer-chain molecules also corresponds to the minimal sorption observed for perfluorobutanoic acid, the shortest chain length in the mixture. This suggests PEI-CDs would be most effective for sorbing longer-chain PFAS containing sulfonate groups.

CONCLUSIONS

In this study, cationic PEI-based carbon dots were designed to sorb environmentally relevant PFAS species. Herein, ^{19}F NMR is demonstrated to be an effective approach to assess association without using any additional sample purification steps. After exposure to PFOA, the PEI-CD effective size increased and ζ -potential decreased, suggesting cationic PEI-CDs sorb negatively charged PFOA. Sorption is further supported by changes to PFOA ^{19}F NMR peak intensity and chemical shifts in the presence of PEI-CDs, both of which are reflective of slow-intermediate exchange kinetics. The peak corresponding to the α -fluorine on PFOA changes the most in

intensity and chemical shift, suggesting electrostatic interactions are likely driving sorption. Time-based studies show that most sorption occurs within the first 2 h of interaction, with no significant changes after 72 h. ^{19}F NMR experiments with a 24-PFAS mixture show PEI-CDs associated with a wide range of PFAS, with a potential preference toward perfluoroalkyl sulfonates and longer-chain species. Overall, PEI-CDs prove to be an effective PFAS sorbent material, and ^{19}F NMR is an effective method to screen for novel sorbent materials and help elucidate interaction mechanisms. These methods not only show a new category of sorbent materials but also serve as a platform for understanding what materials associate with PFAS and how.

MATERIALS AND METHODS

Materials

Citric acid (Sigma-Aldrich, 99.5%), polyethyleneimine (Alfa Aesar, branched, M.W. 10,000, 99%), perfluorooctanoic acid (Sigma-Aldrich, 95%), perfluorobutanoic acid (Sigma-Aldrich, >98%), trifluoroacetic acid-d (99.5 atom % D), and D_2O (Cambridge Isotopes) were used without further purification. DI water was from a Direct-Q 3.5,8 laboratory water purification system by MilliporeSigma. The PFAS mixture was purchased as Native PFAS Reference Standard (M-8327-10X) from AccuStandard containing 24 different components (Table S2).

Synthesis

PEI-based carbon dots (PEI-CDs) were synthesized using branched polyethyleneimine (1.0 g) and citric acid (0.25 g) dissolved in 10 mL of $\text{MQ H}_2\text{O}$ in a CEM Discover SP microwave reactor at 180°C for 4 h (final pH = 9). The product was filtered using a $0.2\ \mu\text{m}$ regenerated cellulose syringe filter to remove bulk carbon residue and further purified with dialysis using Spectra/Por 3 3.5 kD MWCO tubing for 72 h with water changes twice daily. The purified solution was lyophilized for 72 h to obtain a dried yellow-green powder.

Material Characterization of PEI-CDs

The nanoparticle size distribution (DLS) and ζ -potential of carbon dots were determined using Malvern Zetasizer Advance Pro Red. Fluorescence spectra were recorded with a PTI QuantaMaster 400 at an excitation wavelength of 350 nm using 5 nm slit widths from 360 to 600 nm.

Per- and Polyfluorinated Alkyl Substance (PFAS) Exposure Experiments

Dried PEI-CDs were resuspended in MQ water to make a 20 mg/mL stock solution for PFAS exposure experiments. Prior to any PFAS exposure experiments, the stock solution was sonicated for 15 min.

Size, Charge, and Fluorescence. DLS and ζ -potential measurements were conducted on samples prepared with 100 mg/L PEI-CDs and 0 or 5 mg/L PFOA. The pH was adjusted to 4 using 0.1–0.4 M HCl, and samples were left on a shaker for 72 h prior to DLS and ζ -potential measurements. Fluorescence measurements were conducted on samples containing PEI-CDs (500 mg/L) and PFOA (0, 1, 2.5, 5.0, and 7.5 mg/L). The pH was adjusted as above, and samples were left on a shaker for 72 h prior to acquiring the fluorescence spectra. Transmission electron microscopy was conducted using grids prepared with 3 mg/mL of PEI-CDs with a Thermo Fisher Talos F200X operating at 200 keV.

Time-Based Experiments. Time-based experiments were conducted using 100 mg/L PEI-CDs with 5 mg/L PFOA. The pH of the sample was adjusted to 4 using 0.1–0.4 M HCl and immediately prepared for ^{19}F NMR experiments. Spectra were recorded at 12 h increments for 4 days, then once a day until 1 week elapsed. The shortest time point possible is 2 h as that is the acquisition time. The sample remained in the NMR tube for the duration of the experiment. PFOA control spectra were recorded without any PEI-CDs at the beginning and end of the experiment. The change in PFOA peak

integration between the control and PEI-CD-containing solution at each time point was used to assess the timescale of the reaction and determine the best time point to conduct affinity studies.

PFOA Affinity. Samples containing PEI-CDs (0, 0.1, 1, 5, 10, 50, 100, 500, 1000, 5000, and 10000 mg/L) and PFOA (5 mg/L) were prepared in glass scintillation vials with polyethylene caps. The pH was adjusted to 4 using 0.1–0.4 M HCl, and samples were left on a shaker for 72 h ahead of spectral interrogation.

PFAS Mixture. For PFAS mixture experiments, samples were prepared to yield final concentrations of 0, 5, 50, 500, 5000, and 10,000 mg/L PEI-CDs. The pH was adjusted to 4 using 0.1–0.4 M HCl. The PFAS mixture and pH-adjusted PEI-CD solutions were combined to yield the listed PEI-CD concentrations and 5 mg/L PFAS mixture, where each of the 24 components was at 5 mg/L. pH adjustment was done prior to adding PFAS to minimize potential PFAS contamination to lab equipment. Samples were left on a shaker for 72 h ahead of spectral interrogation.

¹⁹F NMR Spectroscopy

All NMR samples were prepared with 90% aqueous sample solution and 10% D₂O (90/10, v/v). A sealed capillary tube containing 50 μM trifluoroacetic acid-d was added to the NMR tube and used as a chemical shift reference (−75.51 ppm).⁴¹ ¹⁹F NMR spectra were acquired at 564 MHz on a Bruker 600-MHz Avance NEO with a 5 mm triple resonance cryoprobe without proton decoupling. A delay time of 8 s and 1024 scans were experimentally determined to give a sufficient signal-to-noise ratio and complete longitudinal relaxation.

Spectral processing was done using MestReNova. Each spectrum was phase-corrected, baselined (Whittaker Smoother), and referenced to TFA at −75.51 ppm. Integration, chemical shift, and peak height were recorded for each fluorine peak of PFOA at all PEI-CDs concentrations. As PEI-CD concentration increased, the concentration of CD-bound PFOA increased, resulting in changes to the ¹⁹F NMR signal. The observed signal intensity change can be assumed to be relatively proportional to the fraction bound (f_b) of PFOA as: $f_b = 1 - f_f = 1 - I_{free}/I_0 = [PFOA-CD]/[PFOA]$, where $[PFOA]$ is the total concentration of PFOA and $[PFOA-CD]$ is the concentration of CD-bound PFOA.²² I_{free} is the PFOA NMR signal of free PFOA at each PEI-CD concentration point, and I_0 is the signal of PFOA without PEI-CDs present. Binding curves were created for each fluorine atom on PFOA using the approximation of the fraction bound ($1 - I_{free}/I_0$) based on integration values and peak height versus mass ratio (M) of PEI-CD:PFOA. Additionally, the average peak height across all 7 peaks was used to determine an average approximate binding curve. Approximate K_D values were obtained by a nonlinear best fit using GraphPad Prism 8 using the following equation:

$$f_b = 1 - \frac{I_{free}}{I_0} \\ = 0.5 * (M + 1 + \frac{K_D}{[PFOA]} - \sqrt{\left(M + 1 + \frac{K_D}{[PFOA]}\right)^2 - 4M})$$

■ ASSOCIATED CONTENT

Supporting Information

The Supporting Information is available free of charge at <https://pubs.acs.org/doi/10.1021/acsnanoscienceau.3c00022>.

- Additional ¹⁹F NMR spectra and PEI-CD characterization data, binding curves and corresponding K_D values, analytes in the 24-PFAS mixture, and assumptions used in the cost assessment (PDF)

■ AUTHOR INFORMATION

Corresponding Author

Christy L. Haynes – Department of Chemistry, University of Minnesota-Twin Cities, Minneapolis, Minnesota 55455,

United States; orcid.org/0000-0002-5420-5867;

Email: chaynes@umn.edu

Authors

Riley E. Lewis – Department of Chemistry, University of Minnesota-Twin Cities, Minneapolis, Minnesota 55455, United States

Cheng-Hsin Huang – Department of Chemistry, University of Minnesota-Twin Cities, Minneapolis, Minnesota 55455, United States; orcid.org/0009-0004-2523-445X

Jason C. White – The Connecticut Agricultural Experiment Station, The Connecticut Agricultural Experiment Station, New Haven, Connecticut 06511, United States; orcid.org/0000-0001-5001-8143

Complete contact information is available at:

<https://pubs.acs.org/10.1021/acsnanoscienceau.3c00022>

Notes

The authors declare no competing financial interest.

■ ACKNOWLEDGMENTS

This work benefitted from conversations with Drs. Sara L. Nason, Nubia Zuverza-Mena, Sara Thomas, and Vasilis Vasiliou. Financial support for this research was provided by a grant from the National Institute of Environmental Health Sciences, National Institutes of Health (R01ES032712). A portion of the effort from C.-H.H. was supported by the National Science Foundation under the NSF Center for Sustainable Nanotechnology (CHE-2001611), a Center for Chemical Innovation, and a MnDRIVE Environment Seed Grant. Effort from R.E.L. was supported by the Biotechnology Training Grant: NIH T32GM008347. Data for ¹⁹F NMR experiments were collected at the Minnesota NMR Center. Transmission electron microscopy was carried out in the Characterization Facility of the University of Minnesota, which receives partial support from the NSF through the MRSEC (Award Number DMR-2011401) and the authors thank Michael Odlyzko for his effort on this. They also thank Prof. William C.K. Pomerantz for guidance with NMR experiments.

■ REFERENCES

- (1) Krafft, M. P.; Riess, J. G. Per- and polyfluorinated substances (PFASs): Environmental challenges. *Curr. Opin. Colloid Interface Sci.* **2015**, *20*, 192–212.
- (2) Buck, R. C.; Franklin, J.; Berger, U.; Conder, J. M.; Cousins, I. T.; de Voigt, P.; Jensen, A. A.; Kannan, K.; Mabury, S. A.; van Leeuwen, S. P. Perfluoroalkyl and polyfluoroalkyl substances in the environment: terminology, classification, and origins. *Integr. Environ. Assess. Manage.* **2011**, *7*, 513–541.
- (3) Fromme, H.; Tittlemier, S. A.; Volkel, W.; Wilhelm, M.; Twardella, D. Perfluorinated compounds—exposure assessment for the general population in Western countries. *Int. J. Hyg. Environ. Health* **2009**, *212*, 239–270.
- (4) Kissa, E. *Fluorinated Surfactants and Repellents*; Marcel Dekker: New York, NY, 2001; Vol. 97.
- (5) Ross, I.; McDonough, J.; Miles, J.; Storch, P.; Thelakkat Kochunarayanan, P.; Kalve, E.; Hurst, J.; S Dasgupta, S.; Burdick, J. A review of emerging technologies for remediation of PFASs. *Rem. J.* **2018**, *28*, 101–126.
- (6) Ching, C.; Klemes, M. J.; Trang, B.; Dichtel, W. R.; Helbling, D. E. β -Cyclodextrin Polymers with Different Cross-Linkers and Ion-Exchange Resins Exhibit Variable Adsorption of Anionic, Zwitterionic, and Nonionic PFASs. *Environ. Sci. Technol.* **2020**, *54*, 12693–12702.

- (7) Wu, C.; Klemes, M. J.; Trang, B.; Dichtel, W. R.; Helbling, D. E. Exploring the factors that influence the adsorption of anionic PFAS on conventional and emerging adsorbents in aquatic matrices. *Water Res.* **2020**, *182*, No. 115950.
- (8) Zhang, D. Q.; Zhang, W. L.; Liang, Y. N. Adsorption of perfluoroalkyl and polyfluoroalkyl substances (PFASs) from aqueous solution - A review. *Sci. Total Environ.* **2019**, *694*, No. 133606.
- (9) Park, M.; Wu, S.; Lopez, I. J.; Chang, J. Y.; Karanfil, T.; Snyder, S. A. Adsorption of perfluoroalkyl substances (PFAS) in groundwater by granular activated carbons: Roles of hydrophobicity of PFAS and carbon characteristics. *Water Res.* **2020**, *170*, No. 115364.
- (10) Stebel, E. K.; Pike, K. A.; Nguyen, H.; Hartmann, H. A.; Klonowski, M. J.; Lawrence, M. G.; Collins, R. M.; Hefner, C. E.; Edmiston, P. L. Adsorption of short-chain to long-chain perfluoroalkyl substances using swellable organically modified silica. *Environ. Sci.: Water Res. Technol.* **2019**, *5*, 1854–1866.
- (11) Li, H.; Kang, Z.; Liu, Y.; Lee, S.-T. Carbon nanodots: synthesis, properties and applications. *J. Mater. Chem.* **2012**, *22*, 24230–24253.
- (12) Zheng, X. T.; Ananthanarayanan, A.; Luo, K. Q.; Chen, P. Glowing graphene quantum dots and carbon dots: properties, syntheses, and biological applications. *Small* **2015**, *11*, 1620–1636.
- (13) Yao, X.; Lewis, R. E.; Haynes, C. L. Synthesis Processes, Photoluminescence Mechanism, and the Toxicity of Amorphous or Polymeric Carbon Dots. *Acc. Chem. Res.* **2022**, *55*, 3312–3321.
- (14) Liu, W.; Li, C.; Ren, Y.; Sun, X.; Pan, W.; Li, Y.; Wang, J.; Wang, W. Carbon dots: surface engineering and applications. *J. Mater. Chem. B* **2016**, *4*, 5772–5788.
- (15) Fan, J.; Claudel, M.; Ronzani, C.; Arezki, Y.; Lebeau, L.; Pons, F. Physicochemical characteristics that affect carbon dot safety: Lessons from a comprehensive study on a nanoparticle library. *Int. J. Pharm.* **2019**, *569*, No. 118521.
- (16) Wang, W.-R.; Chen, P.-Y.; Deng, J.; Chen, Y.; Liu, H.-J. Carbon-dot hydrogels as superior carbonaceous adsorbents for removing perfluorooctane sulfonate from water. *Chem. Eng. J.* **2022**, *435*, No. 135021.
- (17) Nakayama, S. F.; Yoshikane, M.; Onoda, Y.; Nishihama, Y.; Iwai-Shimada, M.; Takagi, M.; Kobayashi, Y.; Isobe, T. Worldwide trends in tracing poly- and perfluoroalkyl substances (PFAS) in the environment. *TrAC, Trends Anal. Chem.* **2019**, *121*, No. 115410.
- (18) Camdzic, D.; Dickman, R. A.; Joyce, A. S.; Wallace, J. S.; Ferguson, P. L.; Aga, D. S. Quantitation of Total PFAS Including Trifluoroacetic Acid with Fluorine Nuclear Magnetic Resonance Spectroscopy. *Anal. Chem.* **2023**, *95*, 5484–5488.
- (19) Wang, A.; Vangala, K.; Vo, T.; Zhang, D.; Fitzkee, N. C. A. Three-Step Model for Protein–Gold Nanoparticle Adsorption. *J. Phys. Chem. C* **2014**, *118*, 8134–8142.
- (20) Zhi, B.; Yao, X.; Wu, M.; Mensch, A.; Cui, Y.; Deng, J.; Duchimaza-Heredia, J. J.; Trerayapiwat, K. J.; Niehaus, T.; Nishimoto, Y.; Frank, B. P.; Zhang, Y.; Lewis, R. E.; Kappel, E. A.; Hamers, R. J.; Fairbrother, H. D.; Orr, G.; Murphy, C. J.; Cui, Q.; Haynes, C. L. Multicolor polymeric carbon dots: synthesis, separation and polyamide-supported molecular fluorescence. *Chem. Sci.* **2021**, *12*, 2441–2455.
- (21) Buchholz, C. R.; Pomerantz, W. C. K. ¹⁹F NMR viewed through two different lenses: ligand-observed and protein-observed ¹⁹F NMR applications for fragment-based drug discovery. *RSC Chem. Biol.* **2021**, *2*, 1312–1330.
- (22) Matei, E.; Andre, S.; Glinschert, A.; Infantino, A. S.; Oscarson, S.; Gabius, H. J.; Gronenborn, A. M. Fluorinated carbohydrates as lectin ligands: dissecting glycan-cyanovirin interactions by using ¹⁹F NMR spectroscopy. *Chemistry* **2013**, *19*, 5364–5374.
- (23) Mishra, N. K.; Urlick, A. K.; Ember, S. W.; Schonbrunn, E.; Pomerantz, W. C. Fluorinated aromatic amino acids are sensitive ¹⁹F NMR probes for bromodomain-ligand interactions. *ACS Chem. Biol.* **2014**, *9*, 2755–2760.
- (24) Shortridge, M. D.; Hage, D. S.; Harbison, G. S.; Powers, R. Estimating protein-ligand binding affinity using high-throughput screening by NMR. *J. Comb. Chem.* **2008**, *10*, 948–958.
- (25) Tengel, T.; Fex, T.; Emtenas, H.; Almqvist, F.; Sethson, I.; Kihlberg, J. Use of ¹⁹F NMR spectroscopy to screen chemical libraries for ligands that bind to proteins. *Org. Biomol. Chem.* **2004**, *2*, 725–731.
- (26) Fedorenko, M.; Alesio, J.; Fedorenko, A.; Slitt, A.; Bothun, G. D. Dominant entropic binding of perfluoroalkyl substances (PFASs) to albumin protein revealed by ¹⁹F NMR. *Chemosphere* **2021**, *263*, No. 128083.
- (27) Weiss-Errico, M. J.; Ghiviriga, I.; O’Shea, K. E. ¹⁹F NMR Characterization of the Encapsulation of Emerging Perfluoroether-carboxylic Acids by Cyclodextrins. *J. Phys. Chem. B* **2017**, *121*, 8359–8366.
- (28) Weiss-Errico, M. J.; O’Shea, K. E. Detailed NMR investigation of cyclodextrin-perfluorinated surfactant interactions in aqueous media. *J. Hazard. Mater.* **2017**, *329*, 57–65.
- (29) Trang, B.; Li, Y.; Xue, X. S.; Ateia, M.; Houk, K. N.; Dichtel, W. R. Low-temperature mineralization of perfluorocarboxylic acids. *Science* **2022**, *377*, 839–845.
- (30) Bhat, A. P.; Mundhenke, T. F.; Whiting, Q. T.; Peterson, A. A.; Pomerantz, W. C. K.; Arnold, W. A. Tracking Fluorine during Aqueous Photolysis and Advanced UV Treatment of Fluorinated Phenols and Pharmaceuticals Using a Combined ¹⁹F-NMR, Chromatography, and Mass Spectrometry Approach. *ACS Environ. Au* **2022**, *2*, 242–252.
- (31) Camdzic, D.; Dickman, R. A.; Aga, D. S. Total and class-specific analysis of per- and polyfluoroalkyl substances in environmental samples using nuclear magnetic resonance spectroscopy. *J. Hazard. Mater. Lett.* **2021**, *2*, No. 100023.
- (32) Ateia, M.; Attia, M. F.; Maroli, A.; Tharayil, N.; Alexis, F.; Whitehead, D. C.; Karanfil, T. Rapid Removal of Poly- and Perfluorinated Alkyl Substances by Poly(ethylenimine)-Functionalized Cellulose Microcrystals at Environmentally Relevant Conditions. *Environ. Sci. Technol. Lett.* **2018**, *5*, 764–769.
- (33) Jiang, B.; Yang, H.; Guo, Y.; Liu, C.; Song, H.; Zhou, P.; Zhang, H.; Zhou, K.; Guo, Y.; Chen, H. Developing electropositive citric acid–polyethylenimine carbon quantum dots with high biocompatibility and labeling performance for mesenchymal stem cells in vitro and in vivo. *New J. Chem.* **2022**, *46*, 2508–2517.
- (34) Muir, D.; Miaz, L. T. Spatial and Temporal Trends of Perfluoroalkyl Substances in Global Ocean and Coastal Waters. *Environ. Sci. Technol.* **2021**, *55*, 9527–9537.
- (35) Gee, C. T.; Arntson, K. E.; Urlick, A. K.; Mishra, N. K.; Hawk, L. M.; Wisniewski, A. J.; Pomerantz, W. C. Protein-observed ¹⁹F-NMR for fragment screening, affinity quantification and druggability assessment. *Nat. Protoc.* **2016**, *11*, 1414–1427.
- (36) Gossert, A. D.; Jahnke, W. NMR in drug discovery: A practical guide to identification and validation of ligands interacting with biological macromolecules. *Prog. Nucl. Magn. Reson. Spectrosc.* **2016**, *97*, 82–125.
- (37) Williamson, M. P. Using chemical shift perturbation to characterise ligand binding. *Prog. Nucl. Magn. Reson. Spectrosc.* **2013**, *73*, 1–16.
- (38) Xu, J.; Liu, Z.; Zhao, D.; Gao, N.; Fu, X. Enhanced adsorption of perfluorooctanoic acid (PFOA) from water by granular activated carbon supported magnetite nanoparticles. *Sci. Total Environ.* **2020**, *723*, No. 137757.
- (39) Qu, Y.; Zhang, C.; Li, F.; Bo, X.; Liu, G.; Zhou, Q. Equilibrium and kinetics study on the adsorption of perfluorooctanoic acid from aqueous solution onto powdered activated carbon. *J. Hazard. Mater.* **2009**, *169*, 146–152.
- (40) Lundquist, N. A.; Sweetman, M. J.; Scroggie, K. R.; Worthington, M. J. H.; Esdaile, L. J.; Alboaiji, S. F. K.; Plush, S. E.; Hayball, J. D.; Chalker, J. M. Polymer Supported Carbon for Safe and Effective Remediation of PFOA- and PFOS-Contaminated Water. *ACS Sustainable Chem. Eng.* **2019**, *7*, 11044–11049.
- (41) Rosenau, C. P.; Jelier, B. J.; Gossert, A. D.; Togni, A. Exposing the Origins of Irreproducibility in Fluorine NMR Spectroscopy. *Angew. Chem., Int. Ed.* **2018**, *57*, 9528–9533.